Phonon spectra in SiO_2 glasses

J.F. Pérez-Robles,[1,2] S. Jiménez-Sandoval,[1] J. González-Hernández,[1] Yuri V. Vorobiev,[1] J.R. Parga Torres,[2] and M.A. Hernández-Landaverde[1]

[1] *Centro de Investigación y de Estudios Avanzados del Instituto Politécnico Nacional Laboratorio de Investigacion en Materiales, Facultad de Química, Centro Universitario Cerro de las Campanas, Universidad Autónoma de Querétaro Querétaro, Mexico*

[2] *Instituto Tecnológico de Saltillo, Departamento de Metal-Mecánica, Blvd. V. Carranza 2400, Saltillo, Coah., Mexico*

Recibido el 27 de enero de 1998; aceptado el 21 de octubre de 1998

Phonon spectra in SiO_2 sol-gel made glasses annealed under different conditions are investigated using infrared absorption and Raman scattering. These data are compared with those obtained in commercial optical-quality quartz. All the materials exhibit the same phonon bands, the exact position and the intensity depend on the measuring technique and on the sample preparation method. The phonon spectra in this material are interpreted on the basis of a simple quasi-linear description of elastic waves in an O-Si-O chain. It is shown that the main features observed in the range 400–1400 cm^{-1} can be predicted using a quasi-linear chain model in which the band at 1070 cm^{-1} is assigned to the longitudinal optical waves in the O-Si-O chain with the smallest possible wavelength at the Brillouin zone boundary, the band located around 450 cm^{-1} is assigned to the transversal optical waves and the band at 800 cm^{-1} to the longitudinal acoustical waves with the same wavelength. The degree of structural disorder can be also deduced within the framework of the proposed model.

Keywords: Sol-gel glasses; phonon spectra; infrared and Raman spectra

Por medio de espectroscopía infrarroja (IR) y Raman se investigó el espectro de fonones en vidrios de SiO_2 producidos por el proceso sol-gel y tratados en diferentes condiciones. Se compararon los datos con aquellos obtenidos sobre cuarzo de calidad óptica. Todos los materiales exhiben las mismas bandas de fonones; sin embargo, la posición exacta y la intensidad dependen de la técnica de medición y del método de preparación de la muestra. El espectro de los fonones en este material se interpreta tomando como base la descripción cuasi-lineal de ondas elásticas en una cadena de O-Si-O. Se muestra que los principales aspectos observados en el intervalo de 400 a 1400 cm^{-1} se pueden predecir usando el modelo de la cadena cuasi-lineal, en el cual la banda a 1070 cm^{-1} se asigna a las ondas ópticas longitudinales en la cadena de O-Si-O con la longitud de onda más pequea posible en la zona de Brillouin. La banda localizada alrededor de 450 cm^{-1} se asigna a las ondas ópticas transversales y la banda en 800 cm^{-1} a las ondas acústicas de la misma longitud de onda. A partir del modelo propuesto se puede obtener información sobre el grado de desorden dentro de la red.

Descriptores: Vidrios sol-gel; espectro de fonones; espectros Raman e infrarrojo

PACS: 61.43.Fs, 78.30.Ly

1. Introduction

Phonon spectra in SiO_2 glasses have been the subject of particular interest during the last decades. Both theoretical and experimental works have shown that certain features in the vibrational spectra could be a source of information about the structure, composition and the degree of structural disorder in these materials [1–8]. Previous calculations of the phonon spectra in vitreous SiO_2 have been based on quasi-crystalline models [6, 7]; on large scale disordered networks [8–10] and on molecular cluster models [11–13]. Previous experimental investigations made on quartz and on other types of amorphous SiO_2 materials prepared by different techniques have shown that the main features in the phonon spectra are the same for all these materials [11–17]. However, the nature of certain bands in the spectra is still not quite clear. For example, the infrared absorption bands centered around 450, 800, and 1070 cm^{-1}, were assigned [18–20] to the rocking, bending and stretching vibrations of the Si-O bond, respectively. Many other papers have been devoted to understanding the origins of these modes and to assigning the corresponding atomic motions [3, 4, 18–23]. At the same time, the main feature in the Raman spectrum of vitreous SiO_2 at 455 cm^{-1} [22] has been assigned to the bond-bending vibration [22].

It should be mentioned, that most of the cited papers give a description of the different vibrational modes using the molecular cluster approximation, *i.e.*, considering a motion of, for example, an oxygen atom under the action of the elastic forces caused by the deformation of the two adjacent bonds. This description could lead to wrong conclusions in a solid, where perhaps the wave approximation could be a more realistic and therefore could provide a more complete picture of the vibrational spectra.

In addition, there has been a lot of controversy in relation to how the degree of structural disorder in vitreous SiO_2 is related to certain features in the phonon spectra measured by spectroscopic techniques [1–5, 21–23]. Some works use the relative intensity of certain bands or their widths to estimate the degree of disorder, perhaps a better way to do that is to use the integrated area under the corresponding bands. In any way, no model has been proposed so far to relate unambiguously the glass structural disorder with the characteristics of the phonon spectra.

In the present study we compare the phonon spectra measured on pure and doped SiO_2 samples obtained using the sol-gel method with that obtained in optical quality quartz. In the doped sol-gel made samples, copper impurities have been added and the samples treated at various temperatures with the intention to modify the structural disorder and therefore to be able to establish a relation between certain features observed in the IR spectra and the degree of structural disorder in these materials. The analysis is made on the basis of a simple description of elastic waves in a quasi-linear O-Si-O chain, this chain being the main constituent of the glass network. The results of this analysis give a reasonably good description of the behavior of the different phonon bands. In addition, it provides a model that correlates the shape of the phonon spectra with the structural disorder in these materials.

2. Materials and methods

The sol-gel samples were prepared by mixing the starting solutions composed of tetraethylorthosilicate (TEOS), water and ethanol. The ethanol to TEOS and water to TEOS molar ratios were 4:1 and 11.7:1, respectively. The copper was introduced into the solution in the form of nitrate. To catalyze the hydrolysis/condensation reactions, a small amount of nitric acid was added. After mixing, the solution was placed in a closed stainless steel container in a constant temperature bath at 35°C. At these conditions the solution viscosity gradually increased reaching solidification at about 36 hours. Powdered samples were obtained after grinding the pieces of solid glass. Further details about the sol-gel method can be found elsewhere [24, 25]. Some samples were heat treated under oxidizing or reducing conditions depending upon the annealing atmosphere (air or CO, respectively). The Raman spectra were obtained using a Micro-Raman system with the 632.8 nm laser light as excitation source and with typical power densities of 10 W/cm^2. The IR absorption spectra were obtained with a FT-IR spectrometer Perkin Elmer System model 2000, used it in the diffuse reflectance mode.

3. Experimental spectra

Figure 1 shows a typical IR absorption spectrum in the range of 400–1700 cm^{-1} (curve 1), the Raman spectrum for a sol-gel sample (curve 2) and the Raman spectrum for commercial optical quality quartz slide (curve 3). The majority of

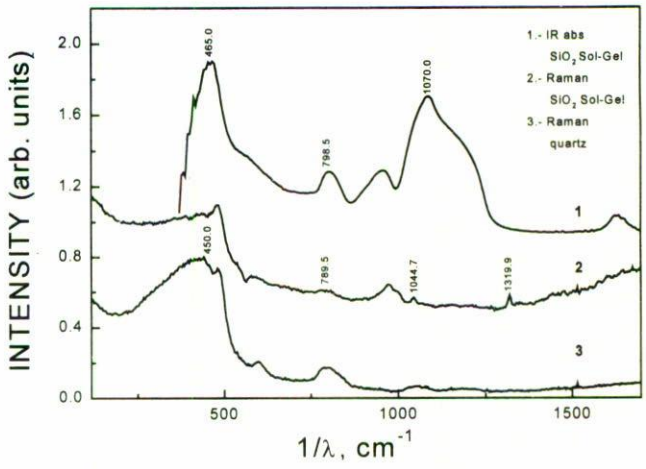

FIGURE 1. IR absorption spectrum from 400 to 1700 cm^{-1} (curve 1), Raman spectrum for a sol-gel sample (curve 2) and Raman spectrum for a commercial optical quality quartz slide (curve 3).

the bands usually observed are present in the three spectra, although the intensity ratio of the different bands varies from sample to sample. These bands related to vibrations of the Si-O network are located at about 450, 800, and 1070 cm^{-1}. The latter band is composed of several features which include bands at around 1070, 1160, and 1215 cm^{-1}, as reported in previous papers, assigned to the TO_3, LO_4 and TO_4 modes, respectively [4]. In curve 2 an additional band at about 1320 cm^{-1} is observed. This band was previously observed in the IR spectra of sol-gel made samples with low percentage of water in the initial solution. This condition produces glass not normally structured presenting well-defined Si-O-Si chains but not properly interconnected. Notice that this band does not appear in the Raman spectrum of the quartz sample, therefore this line originates from structural disorder.

At this point, we will restrict our discussion to the three bands at about 450, 800, and 1070 cm^{-1}. The effects due to disorder will be discussed in a subsequent section. Table I summarizes the detailed position of the bands located around 800, and 1070 cm^{-1}, as obtained by IR and Raman measurements, for several samples produced by the sol-gel method. The exact position of each band depends on the sample, but there is some correlation between the shifts of the different bands: if the band centered around 1070 cm^{-1} moves to a certain direction, the band around 800 cm^{-1} moves towards the same direction whereas the 450 cm^{-1} band moves to the opposite one, this may be observed in the spectra of Fig. 1. This behavior is not consistent with the assumption that the band at 800 cm^{-1} corresponds to the bond-bending deformation because in such case its frequency ought to be proportional to $\cos(\theta/2)$ (θ being the Si-O-Si angle, see the figures and considerations in the next section), whereas the frequency of the bond-stretching vibration (1050–1080 cm^{-1}) is proportional to $\sin(\theta/2)$. Therefore, any variation of θ in different samples should shift these bands in opposite direc-

TABLE I. Vibrational frequencies for the indicated bands and related data for different SiO_2 glasses (s.g. = sol-gel).

Sample	Treatment	Spectra	ω_0 (cm^{-1})	ω' (cm^{-1})	ω'/ω_0
s.g. SiO_2	500°C, ox.	IR	1051.2	798.5	0.760
SiO_2, Corning glass	None	Raman	1071.5	803.5	0.750
s.g. SiO_2	300°C, red	Raman	1044.7	789.5	0.756
quartz	None	Raman	1048.0	786.1	0.750
s.g. SiO_2(0.3CuO)	800°C, red	IR	1077.8	811.2	0.753
s.g. SiO_2(0.3CuO)	500°C, red	IR	1081.2	808.7	0.758
s.g. SiO_2(0.3CuO)	300°C, red	IR	1073.8	806.7	0.750
s.g. SiO_2(0.6CuO)	800°C, red	IR	1083.6	814.7	0.752
s.g. SiO_2(0.6CuO)	500°C, red	IR	1074.3	806.3	0.751
s.g. SiO_2	100° C, ox.	Raman	1044.7	789.5	0.756
s.g. SiO_2(0.6CuO)	800° C, red	Raman	1085.0	813.5	0.750
s.g. SiO_2(0.3Fe_2O_3)	500°C, red	IR	1065.0	801.0	0.752

$\langle\omega'\rangle = 802.4$, standard deviation = 9.75, relative dispersion 1.2%
$\langle\omega_0\rangle = 1066.7.$, standard deviation =15.5, relative dispersion 1.45%
$\langle\omega'/\omega_0\rangle = 0.753$, standard deviation = 0.0035, relative dispersion 0.46%

tions [11]. These observations lead us to accept the conclusion obtained in Ref. 11 in which the main Raman band around 450 cm^{-1} corresponds to bond-bending vibrations. This conclusion agrees well with the behavior observed in such bands when structural changes in the samples are induced by either doping or annealing and with the value of the O-Si-O angle $\theta \approx 135°$ [for which $\sin(\theta/2)/\cos(\theta/2) = 2.4$, and 1070/450 = 2.38]. The nature of the band at 800 cm^{-1} will be discussed later in this paper. We could also mention that the so-called bond-rocking atomic motion frequently mentioned in literature does not, in a first approximation, produce any bond deformation and, therefore, should not give an oscillation mode at all. The band at about 900 cm^{-1} in spectra 1 and 2 is due to the stretching vibration of the silanol group (Si-OH).

4. Phonon spectra in a quasi-linear O-Si-O chain

To obtain a general description of the phonon spectra in SiO_2 glasses, a simple calculation has been carried out for elastic waves traveling in a quasi-linear O-Si-O chain. We have followed the standard procedure employed to calculate the phonon dispersion relation in a diatomic chain. It is expected that this approximation could provide a reasonable approach to the three-dimensional case for at least the longitudinal waves when the atomic motion in one chain causes only a small perturbation to the neighbor chains.

Figure 2A shows a schematic view of the Si-O-Si-O chain where the open and closed circles represent the oxygen and the silicon atoms, respectively. It is generally accepted that this chain is the main constituent of the glass network and that

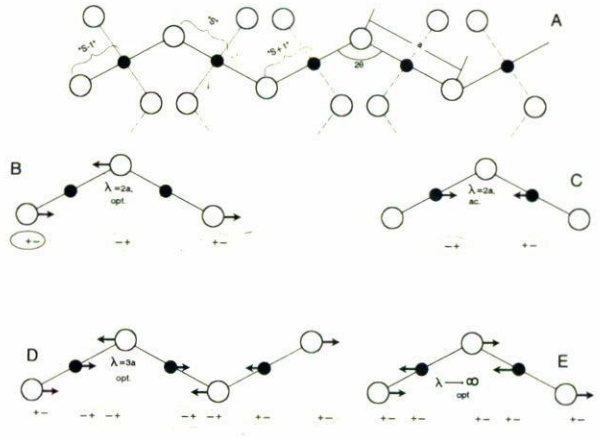

FIGURE 2. Schematic view of the Si-O-Si-O chain (A) and d isplacements along the chain of the O- and Si-atoms (B–E).

the length of the chain will depend on the degree of structural disorder in the glass. In this calculation we have assumed a periodic infinite chain, leaving the effects of disorder for the next section. The Newtonian equations for the longitudinal motion of the two atoms in the cell number s are

$$m_{\mathrm{O}} \frac{d^2 u_s}{dt^2} = k\,(v_s + v_{s-1} - 2u_s)\sin^2\frac{\theta}{2}, \qquad (1)$$

$$m_{\mathrm{Si}} \frac{d^2 v_s}{dt^2} = k\,(u_s + u_{s+1} - 2v_s)\sin^2\frac{\theta}{2}, \qquad (2)$$

where $m_{\mathrm{O,Si}}$ are the masses of the oxygen and silicon atoms, k is the elastic coefficient of the stretching bond, and u and v are the displacements along the chain (see Fig. 2B–2E) of the O- and Si-atoms, respectively.

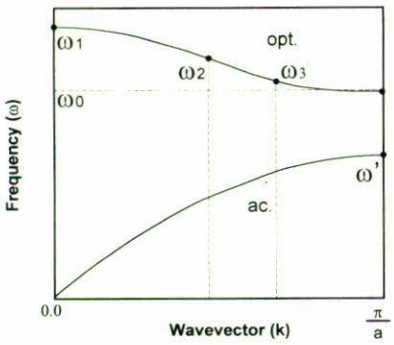

FIGURE 3. Solution of the Eq. (5) for the optical and acoustical phonons.

We employ oscillatory solutions of the form:

$$u_s = u \exp i(Kas - \omega t),$$
$$v_s = v \exp i(Kas - \omega t),$$

a being the lattice constant of the chain, and obtain the system of equations

$$-\omega^2 m_O\, u = \alpha v[1 + \exp(-iKa)] - 2\alpha u, \quad (3)$$
$$-\omega^2 m_{Si}\, v = \alpha u[1 + \exp iKa] - 2\alpha v \quad (4)$$

where $\alpha = k\sin^2(\theta/2)$.

Solving the quadratic equations above, it is obtained the equation for ω

$$\omega^4 - 2\alpha \frac{m_O + m_{Si}}{m_O m_{Si}} \omega^2 + \frac{2\alpha^2}{m_O m_{Si}} (1 - \cos Ka) = 0. \quad (5)$$

Equation (5) gives the phonon dispersion law for a quasi-linear chain, *i.e.* the dependence of the frequency ω upon the wave vector $K = 2\pi/\lambda$, (λ being the wavelength). A simple analysis [26] shows that Eq. (5) gives two branches, one for the optical and another for the acoustical phonons (see Fig. 3); some important phonons in the dispersion curves are the following:

a) Small K (the wavelength $\lambda \gg a$, $K \approx 0$); the optical frequency is given by

$$\omega_{opt}^2 = \omega_1^2 = 2\alpha \frac{m_O + m_{Si}}{m_O m_{Si}} = 1.57\omega_0^2,$$

where we denote

$$\omega_0 = \sqrt{2\alpha/m_O}. \quad (6)$$

So,

$$\omega_1 = 1.252\omega_0. \quad (7)$$

The acoustical branch near $K = 0$ is approximately linear:

$$\omega_{ac} = K[\alpha/2(m_O + m_{Si}]^{0.5} a$$

b) K has the highest possible value (zone edge) $K = K_{max} = \pi/a$ ($\alpha = 2a$ see Fig. 2B and 2C). In this case,

$$\omega_{opt} = \omega_0,$$
$$\omega_{ac} = \omega' = \left(\frac{2\alpha}{m_{Si}}\right)^{0.5} = \omega_0 \sqrt{\frac{m_O}{m_{Si}}} = 0.756\omega_0. \quad (8)$$

c) $K = 2/3K_{max}$, the wavelength $\lambda = 3a$ (see Fig. 2D)

$$\omega_3 = 1.104\omega_0. \quad (9)$$

d) $K = 0.5K_{max}$, $\lambda = 4a$

$$\omega_2 = 1.167\omega_0. \quad (10)$$

Now we see that if one takes $\omega_0 = 1065\ cm^{-1}$, the values for $\omega_{3,2,1} = 1174$, 1244, and 1330 cm^{-1} can be obtained, respectively. As pointed out before in the text, the bands ω_0, ω_3, and ω_2 have been previously reported and attributed to the TO_3, LO_4 and TO_4 modes respectively, the last one is observed in the Raman spectra of Fig. 1. From this approach, all the bands observed in the range 1000–1350 cm^{-1} correspond to different optical phonons of the longitudinal branch and all are of the LO-type.

The density of states in K-space is uniform, therefore, the highest density of states corresponds to the flat parts of the dispersion curves (*i.e.* is observed for ω_0, ω_1 and ω'). From Figs. 2B–2E one observes that all phonons, except those with $\lambda = 2a(\omega = \omega')$, are accompanied by the motion of Si-atoms, which will result in some dissipation of vibrational energy due to the interconnection with the surrounding O-Si-O chains. For that reason the intensity of the infrared band corresponding to $\omega = \omega_0$ is dominant.

The band around 800 cm^{-1} is assigned to the acoustic phonons with the highest wave vector ($\lambda = 2a$, $\omega = \omega'$). As it is evident from the Table I, the ratio ω'/ω_0 is very close to the theoretical value given by Eq. (8), and its relative dispersion less than 0.5%, which is much smaller than the dispersion of the values for ω_0 and ω' which are 1.5 and 1.2%, respectively. This means that some correlation exists between the values of ω_0 and ω', in agreement with our considerations.

For the transversal waves, that is, for atomic displacements normal to those shown in Fig. 2, a similar approach will produce a dispersion law of the same kind, but with a scaling factor proportional to $\cos(\theta/2)$ instead of $\sin(\theta/2)$. It is easy to see that the wave numbers between 1070 and 1320 cm^{-1} being divided by the factor $\sin(\theta/2)\cos(\theta/2) = 2.4$ would give the values 446–550 cm^{-1} which correspond to the main Raman bands observed in this material. But we do not attempt to make a detailed analysis of this region since the applicability of the quasi-linear approach to this case is not quite justified.

5. Glass disorder effects

The relative intensities of the different bands could be estimated if we find the effective dipole momentum generated by the different vibrations. To do so, we have to know the displacement of the atoms during the propagation of the elastic waves. For this, one uses Eqs. (3) and (4) and finds the relations between the values u, v for the different frequencies. The main results are as follows:

a). For $K \approx 0$, that is $\lambda \to \infty$, introducing the corresponding value of ω given by Eq. (5) in Eq. (3,4), we get:

$$\frac{u}{v} = -\frac{m_{\mathrm{Si}}}{m_{\mathrm{O}}}, \tag{11}$$

which means that the displacements of the oxygen and the silicon atoms are inversely proportional to their masses and have the opposite directions so that the gravity center of the whole system does not change, a general rule for the optical phonons. The atomic displacements for the different vibrations are shown in Fig. 2.

b). For $K = \pi/a$, or $\lambda = 2a$, one obtains the corresponding relations for the optical phonon

$$u = u; \quad \left(\frac{m_{\mathrm{Si}}}{m_{\mathrm{O}}}\right) v = v, \tag{12}$$

which mean that u could have any value whereas v is always zero. For the acoustic wave with the same wavelength the relations would be

$$v = v, \quad \left(\frac{m_{\mathrm{O}}}{m_{\mathrm{Si}}}\right) u = u. \tag{13}$$

So, for optical phonons with $\lambda = 2a$ only the oxygen atoms move, whereas for acoustic mode only the silicon atoms are in motion.

c). For $\lambda = 3a$ one gets the following relation between u and v:

$$\frac{u}{v} = -1.14 + i1.97 = -2.28 \exp\left(\frac{-i\pi}{3}\right) \tag{14}$$

indicating a phase shift in the motion of the two different atoms (see Fig. 2D).

Taking the oxygen and silicon atoms as negative and positive charges, respectively, the resulting distribution of charge along the chain induced by the atomic displacements is shown in Fig. 2. The positions of the atoms are denoted by its charge, while the equilibrium positions show the deficit of the corresponding charge. Thus, the atomic displacements originate the appearance of the charges as indicated in the figure. One can see that for both optical and acoustical phonons with $\lambda = 2a$, there appear a series of pairs of identical dipoles with opposite orientation, resulting in a net dipole moment equal to zero. It could be observed that for $\lambda = 4a$ the situation is the same (not shown in Fig. 2). In the case $\lambda = 3a$ the orientation of the adjacent dipoles is opposite but they are not compensating each other, resulting in a non vanishing dipole moment. This means that the bands corresponding to the phonons with $\lambda = 2a$ and $4a$ in the ordered material, *i.e.*

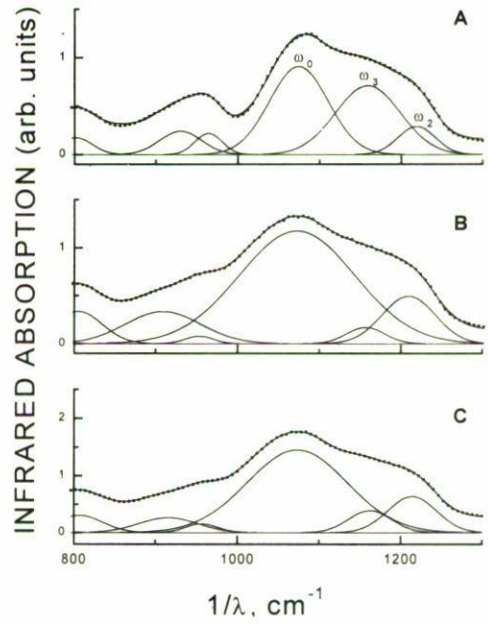

FIGURE 4. Areas of the different bands in the stretching region of the IR spectra for sol-gel samples for different impurities and heat treatments. Measured spectra in continuous line and different bands of the deconvoluted spectra in dotted line. Figure A corresponds to the undoped sample.

with long chains, couple weakly with the electromagnetic radiation and therefore weak band intensities should be observed. The disorder violates the compensation of the dipoles with opposite momentum, thus increasing the intensities of the corresponding bands with the frequencies ω', ω_0 and ω_2. In this approach the band ω_3 should be the least sensitive to the disorder.

In order to have an experimental evaluation of the discussed effects, we compared the areas of the different bands, in the stretching region of the IR spectra of the sol-gel made samples, having different impurities and heat treated at different conditions. The continuous line shows the measured spectra in Fig. 4. It has been deconvoluted in several bands that include the bands corresponding to ω_0, ω_2 and ω_3. In this figure, the dotted curve is the sum of the various features composing the bond-stretching region, as can be observed the dotted and experimental curves are very similar, indicating an appropriated decomposition. Figure 4A corresponds to an undoped sample annealed at 100°C. We expect this sample to have the least degree of disorder. In this case, the ratio of the areas under the two bands at ω_0 and ω_3 is 1.2 and, according to our scheme mentioned above, this ratio should increase with increasing of the degree of disorder.

The spectrum shown in Fig. 4B corresponds to a copper-doped sample after being annealed in oxidizing atmosphere at 300°C. In this case the Cu-atoms break into the glass chains [28] substituting the Si atoms at randomly located sites. Thus, the chain length decreases and the degree of disorder increase. The ratio of the areas of the two bands corre-

sponding to the frequencies ω_0 and ω_3 is 21 in this case. Figure 4C corresponds to a sample containing copper annealed in reducing atmosphere at 800°C, in this case the Cu-atoms segregate into the Cu-particles [28] thus partially restoring the glass chains. The corresponding area ratio here is 9. At the same time, the ratio between the areas of the bands corresponding to the frequencies ω_0 and ω_2 is in all three cases around 5.

6. Conclusions

Based on IR and Raman investigations, the phonon bands in SiO_2 samples with different degree of structural disorder have been analyzed. The solution of the dynamic equations in a quasi-linear O-Si-O chain considering the bond-stretching waves in the chain predicts well the frequency position of the main vibrational bands observed in the experimental data. It was so found that all the phonon bands observed in the range 1000–1350 cm^{-1} correspond to different longitudinal optical modes: the one at about 1070 cm^{-1} has the wavelength $\lambda = 2a$ (a is the lattice constant of the chain), for those at about 1175, 1245, and 1330 cm^{-1}, the corresponding wavelengths are $\lambda = 3a$, $4a$ and $\lambda \to \infty$. The band around 800 cm^{-1} originates from the acoustical phonons at the zone edge. The 450 cm^{-1} band was ascribed to the transversal optical modes, which correspond to the bending deformation of the Si-O bonds. The quasi-linear chain model employed in this work is mostly appropiate for analyzing longitudinal modes in systems where such molecular approximation may be applicable.

The overall dipole moment generated by the oscillations mentioned above in an ordered material is the smallest for waves with $\lambda = 2a$ and $\lambda = 4a$. In these cases the material contains equal amounts of micro-dipoles with opposite moment yielding a net dipole moment equal to zero. A non-vanishing dipole moment is obtained when $\lambda = 3a$. Optical activity is originated in the first two cases by disorder, which breaks the symmetry of adjacent dipoles. In this picture the effect of disorder in the last case would be less pronounced. This argument agrees well with the experiment when the ratio of the areas of the involved modes in samples with different degrees of disorder is determined.

Acknowledgments

The authors thank Ing. Francisco Rodríguez Melgarejo for technical assistance and CONACyT (México) for partial financial support.

1. Young-Bae Park, Shi-Woo Rhee, Y. Imaizumi, and T. Urisu, *J. Appl. Phys.* **80** (1996) 1236.
2. P.G. Pal, S.S. Chao, Y. Takagi, and G. Lucovsky, *J. Vac. Sci. Technol.* **A4** (1986) 689.
3. P. Grosse *et al.*, *Appl. Phys.* **A39** (1986) 257.
4. P. Lange, *J. Appl. Phys.* **86** (1989) 201
5. G. Lucovsky, J.T. Fitch, E. Kobeda, and E.A. Irene, "Local atomic structure of thermally grown SiO_2 films", in *The physics and Chemistry of SiO_2, and the Si-SiO_2 Interfaces*, Edited by Robert Helms and B.E. Deal, (Plenum, New York 1988).
6. J.B. Bates, *J. Chem. Phys.* **56** (1972) 1910.
7. J. Bock and G.J. Su, *J. Am. Ceram. Soc.* **53** (1970) 69.
8. R.J. Bell and P. Dean, *Nature* **212** (1966) 1354.
9. R.J. Bell and D.C. Hibbins-Butler, *J. Phys. C* **9** (1976) 1171.
10. R.J. Bell and D.C. Hibbins-Butler, *J. Phys. C* **3** (1970) 2111.
11. P.N. Sen and M.F. Thorpe, *Phys. Rev. B* **15** (1977) 4030.
12. R.B. Laughlin and J.D. Joannopoulos, *Phys. Rev. B* **16** (1977) 2942.
13. G. Lucovky, *Phil., Mag.* **39** (1979) 513.
14. A.G. Revesz and G.E. Walrafen, *J. Non-Cryst. Solids* **54** (1983) 323.
15. F.L. Galeener, *J. Non-Cryst. Solids* **49** (1982) 53.
16. T. Furukawa and William B. White, *J. Non-Cryst. Solids* **38** (1980) 87.
17. G.E. Walrafen and P.N. Krishnan, *J. Chem. Phys.* **74** 8(1981) 532.
18. F. Orgaz and H. Rawson, *J. Non-Cryst. Solids* **82** (1986) 379.
19. J. Wonf, *J. Electron. Mater.* **5** (1976) 113.
20. G. Lucovsky, C.K. Wong, and W.B. Pollard, *J. Non-Cryst. Solids* **59** (1883) 839.
21. F.L. Galeener and G. Lucovsky, *Phys. Rev. Lett.* **37** (1976) 474.
22. F.L. Galeener, *Phys. Rev. B* **19** (1979) 4392.
23. Ian W. Boyd, *Appl. Phys. Lett.* **51** (1987) 418.
24. L.C. Klein (ed.), *Sol-Gel Technology for Thin Films, Fibers, Preforms, Electronics, and Specialty Shapes*, (Noyes Publications, New Jersey, 1988) p. 50.
25. J.L. Vosse, and W. Kern (eds.), *Thin Film Processes II*, (Academic Press, Inc., 1991) p. 501
26. C. Kittel, *Introduction to Solid State Physics*, 5th Edition, (John Wiley and Sons, New York, 1976)
27. H. Schmodt, *J. Non-Cryst. Solids* **82** (1988) 51.
28. J. Gonzalez-Hernandez *et al.*, *Proceedings of SPIE Conference*-1997 (in press)